SOLAR CELL MINORITY CARRIER LIFETIME USING OPEN-CIRCUIT VOLTAGE DECAY

MARTIN A. GREEN

Joint Microelectronics Research Centre, University of New South Wales, Kensington, New South Wales 2033 (Australia)

(Received August 9, 1983; accepted September 5, 1983)

Summary

A simple method used to measure minority carrier lifetimes in solar cells is to forward bias the cell in the dark and to monitor the decay in the voltage across the cell when the forward current is suddenly terminated. Ideally this decay is linear with a slope inversely proportional to the lifetime. While this open-circuit voltage decay method is simple in principle, in practice it tends to be subjective and unreliable because of departures of the observed decay curves from linearity. Interpretation is further complicated by effects such as junction capacitance, junction recombination, shunt resistance, finite cell base width, non-ideal emitter properties and high injection effects. In the present paper, recent theoretical and experimental developments which have significantly improved the reliability and accuracy of the approach are reviewed.

1. Introduction

The open-circuit voltage decay technique [1, 2] is a simple non-destructive method for measuring minority carrier lifetimes in solar cells. The decay of the voltage across an unilluminated cell is observed after the cell which was originally forward biased is suddenly open circuited (Fig. 1). In the simplest case this decay is linear with a slope equal to $kT/q\tau_B$ where τ_B is the lifetime in the base of the cell and kT/q is the thermal voltage.

In practice, the method tends to be subjective and unreliable because of the difficulty which frequently arises in finding a region of the decay which is reasonably linear. Moreover, the interpretation of the measured value is complicated by effects such as junction capacitance, junction recombination, shunt resistance, finite cell base width, non-ideal properties in the emitter of the cell and high injection into the base region. However, there have been recent developments in both experimental [3] and theoretical [4 - 9] areas which have significantly improved the reliability and accuracy of the approach. In the present paper these developments are reviewed and the relevance of the approach, with these improvements, to solar cell measurements is assessed.

0379-6787/84/$3.00

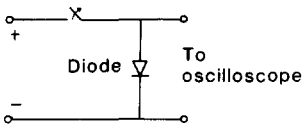

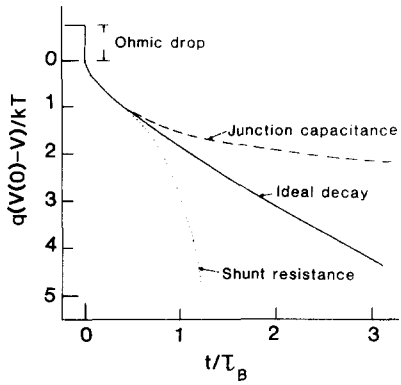

Fig. 1. Schematic illustration of the open-circuit voltage decay method. At $t = 0$ the switch is opened. The decay of the voltage across the cell gives the lifetime in its base.

Fig. 2. Theoretical form of the open-circuit voltage decay for a wide base solar cell.

2. Ideal decay

For a "wide base" solar cell where the thickness W of the base region is much larger than the minority carrier diffusion length L_B, the theoretical expression for the open-circuit voltage decay for $V(t) \gg kT/q$ is [2]

$$V(t) = V(0) - \frac{kT}{q} \ln\left\{\operatorname{erfc}\left(\frac{t}{\tau_B}\right)\right\} \tag{1}$$

where $V(t)$ is the voltage across the cell as a function of time t. Differentiating gives

$$\frac{dV(t)}{dt} = - \frac{(kT/q)\exp(-t/\tau_B)}{(\pi t \tau_B)^{1/2} \operatorname{erfc}\{(t/\tau_B)^{1/2}\}} \tag{2}$$

For $t \gg \tau_B$ this reduces to

$$\frac{dV(t)}{dt} = - \frac{kT/q\tau_B}{1 - \tau_B/2t} \tag{3}$$

From eqns. (2) and (3) it is seen that theory does not predict a simple linear decay as is generally assumed. However, as shown in Fig. 2, after a rapid non-linear initial decay the decay does approach a linear decay with a slope of magnitude $kT/q\tau_B$. Additional insight into the decay mechanism is gained by considering the continuity equation for minority carriers within the cell base region:

$$I_B = \frac{dQ_B}{dt} + \frac{Q_B}{\tau_B} \tag{4}$$

where Q_B is the excess minority carrier charge within the base region and I_B is the current into the base due to minority carrier flows. Under open-

circuit conditions when $I_B = 0$, eqn. (4) shows that the total charge in the base region decays exponentially. The rate of voltage decay can be expressed as

$$\frac{dV}{dt} = -\frac{fkT}{q\tau_B} \tag{5}$$

where

$$f = \frac{q/kT}{d(\ln Q_B)/dV} \tag{6}$$

and is time dependent in general. In the quasi-static approximation, Q_B will depend exponentially on the normalized cell voltage and f will be identically equal to zero. From eqns. (2) and (3) it can be shown that in actuality f will be much higher than unity during the rapid initial regions of the decay but will approach unity at large t.

3. Junction capacitance, junction recombination and shunt resistance

The effects of junction capacitance and junction recombination have been recently analysed by Mahan and Barnes [4]. As shown in Fig. 2, junction capacitance will tend to slow down the open-circuit voltage decay, while junction recombination will act in the same general way as a shunt resistance and will accelerate the voltage decay. All these effects cause a departure from the expected near-linear decay at low voltage levels. In combination with the theoretically expected departure from non-linearity at high voltages, this means that experimentally it is not uncommon to be unable to find any portion of the open-circuit decay curve sufficiently linear for accurate measurements. If a tangent to any given region of the decay curve is selected as being representative of the slope, the lifetime calculated will be overestimated if the junction capacitance dominates the decay curve and underestimated if one of the other effects mentioned above dominates. This is believed to be one of the major reasons for the subjectivity and unreliability of the method.

Mathematically, when the junction capacitance C_J is appreciable, eqn. (4) becomes on open circuit

$$-C_J\frac{dV}{dt} = \frac{dQ_B}{dt} + \frac{Q_B}{\tau_B} \tag{7}$$

with the solution

$$\frac{dV}{dt} = -\frac{f'kT}{q\tau_B}\left(1 + \frac{C_J}{Q_B}\frac{f'kT}{q}\right)^{-1} \tag{8}$$

f' is defined in the same way as f but the two quantities may not be equal for the two different decay conditions. For small t, Q_B is large and the

junction capacitance term in eqns. (7) and (8) may be insignificant. In this case the decay will proceed as before with $f' = f$. However, Q_B decays exponentially with time so that eventually the junction capacitance term will become significant. The whole decay will then slow down as indicated by the broken curve in Fig. 2. It should be noted that f' may differ from f during this phase although both will be close to unity.

The effects of recombination in the junction depletion region and shunt resistance are qualitatively similar. Junction recombination effects are equivalent to those of a non-linear shunt resistance of appropriate magnitude and will not be treated separately. In the presence of a shunt resistance R, eqn. (4) becomes

$$-\frac{V}{R} = \frac{dQ_B}{dt} + \frac{Q_B}{\tau_B} \tag{9}$$

with the solution

$$\frac{dV}{dt} = -\frac{f''kT}{q\tau_B}\left(1 + \frac{V\tau_B}{RQ_B}\right) \tag{10}$$

Again, for small t, Q_B is large so that the shunt resistance term above may be insignificant and the decay will proceed as in the ideal case with $f'' = f$. As Q_B decreases, the shunt resistance term will dominate and the decay will accelerate as indicated by the lower dotted curve in Fig. 2. It should be noted that f'' is unlikely to equal f once this occurs.

Solar cells are particularly vulnerable to the above effects since they are designed to operate at relatively low current densities compared with other semiconductor diodes. Additionally, shunt resistance in solar cells does not have to be particularly high to produce acceptable devices [10]. Cells with low bulk lifetimes or high base doping levels are particularly likely to have their open-circuit decay dominated by capacitive effects. For these reasons the conventional open-circuit voltage decay method is not particularly well suited to measuring minority carrier lifetimes in solar cells.

However, an improved version of the open-circuit voltage decay technique has recently been described which allows the effects described in this section to be compensated [3]. This has been found to improve the reliability and accuracy of the approach greatly.

4. Compensated differential open-circuit voltage decay

The improved technique is based on the observation that junction capacitance and shunt resistance have opposite effects on the open-circuit voltage decay. When both these effects are important, eqn. (4) becomes

$$-\frac{V}{R} - C_J\frac{dV}{dt} = \frac{dQ_B}{dt} + \frac{Q_B}{\tau_B} \tag{11}$$

with the solution

$$\frac{dV}{dt} = -\frac{f^*kT}{q\tau_B}\,\frac{1+(V/R)(\tau_B/Q_B)}{1+(f^*kT/q)(C_J/Q_B)} \tag{12}$$

where f^* is defined in the same way as f in eqn. (6). Since the two terms on the left-hand side of eqn. (11) have opposite signs during voltage decays, it is possible to provide an effective cancellation of these terms over large segments of the voltage decay by augmenting whichever is the smaller. The open-circuit voltage decay then reverts to the ideal solution as given by eqns. (1), (2) and (5).

By examining the differential of the open-circuit voltage decay, it is possible to adjust the degree of cancellation very sensitively as well as to obtain a direct reading of carrier lifetime. Figure 3 is a schematic diagram of the experimental configuration. It differs from Fig. 1 by the addition of a simple passive differentiator formed by the elements C_D and R_D as well as by the capacity to connect a compensation resistance R_C *or* a capacitance C_C in parallel with the diode under test. The differentiator time constant R_DC_D is chosen as about one-tenth of the base lifetime to provide sufficiently fast response and to ensure that the voltage at b is much smaller than that at a.

With R_C and C_C switched out of the circuit, the differentiator output will take the appearance either of the upper or of the lower curve of Fig. 4, depending on whether the shunt resistance or the junction capacitance respectively is dominating the decay. The initial portions of the curve (less than 20 μs) correspond to the relaxation of the differentiator output from its high initial value. This high initial value is due to the loss of the ohmic voltage across the cell immediately after it has been open circuited (Fig. 2). In each case, by adding compensating capacitance and resistance respectively, the decay can be compensated to give the differentiator output shown by the middle curve of Fig. 4. The objective is to obtain a very slight local minimum, in this case at about 60 μs, followed by a very slight local maximum, in this case at about 100 μs. Dividing kT/q by the value of dV/dt at the local minimum will be shown to give a lower bound on the base lifetime, irrespective of the effects to be described in the following sections [3].

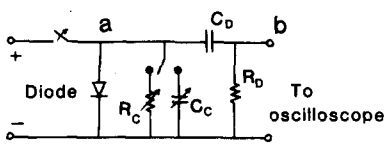

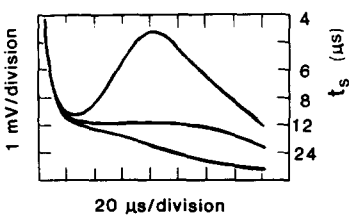

Fig. 3. Experimental arrangement for the compensated differential open-circuit voltage decay method. A passive differentiator formed by R_D and C_D has been added as has the ability to add compensating elements R_C *or* C_C.

Fig. 4. Experimental output from the circuit of Fig. 3 (differentiator time constant RC = 0.95 μs). The top and bottom curves require capacitive and resistive compensation respectively. The middle curve shows a well-compensated waveform.

For the device of Fig. 4 this lower bound is approximately 12 μs. If the effects of the following sections can be correctly assessed for a particular device, an upper bound can also be assigned [3].

The advantage of the compensated differential open-circuit voltage decay technique over the normal technique is that it removes the ambiguity in a given situation as to whether an upper or lower bound is being measured, as well as enabling tighter bounds on the measured lifetime to be determined [3].

5. Finite base width

Several researchers have analysed the effect of finite base width on the open-circuit voltage decay technique [5 - 7]. The clearest conclusions for solar cells have been reached by Jain and coworkers [7].

Irrespective of the effective recombination velocity S of the contact region at the rear of the cell, decreasing the cell base width W increases the linearity of the open-circuit voltage decay. The "lifetime" calculated from the asymptotic value of the decay decreases from τ_B to $\tau_B/(1 + \phi^2)$ where ϕ is the first root of the equation [7]

$$\phi \tan\left(\frac{W\phi}{L_B}\right) = \frac{SL_B}{D_B} \tag{13}$$

where D_B is the minority carrier diffusion coefficient in the base and L_B $(= (D_B\tau_B)^{1/2})$ is the minority carrier diffusion length. Hence, lifetimes calculated without correction will be underestimates when the cell has a base width which is not large compared with minority carrier diffusion lengths.

The most serious underestimates occur when the rear contact to the cell has a high recombination velocity. An "ideal ohmic contact" has in fact an infinite value of this velocity. In such cases the value of lifetime τ_m measured without correction will be less than $4W^2/\pi^2 D_B$. The actual base lifetime τ_B will be given by

$$\frac{1}{\tau_B} = \frac{1}{\tau_m} - \frac{\pi^2 D_B}{4W^2} \tag{14}$$

If the uncorrected value is higher than the previous limit, the rear contact to the cell has a low effective recombination velocity, indicating the presence of back-surface fields or equivalent action. In this case, eqn. (13) must be used to make the appropriate corrections. A simplification occurs when the recombination velocity and/or the base width are (is) very small such that $SW \ll D_B$. In such cases the measured lifetime τ_m will always be less than W/S and the actual base lifetime will be given by

$$\frac{1}{\tau_B} = \frac{1}{\tau_m} - \frac{S}{W} \tag{15}$$

6. Non-ideal emitters

Ideally, the emitter of a solar cell should have unity injection efficiency to maximize the cell open-circuit voltage. In practice, heavy doping effects in the emitter can make the injection efficiency somewhat less than this.

The effect of non-ideal emitter properties has been described in several papers [2, 8, 9]. Analytical solutions have been reported for uniformly doped emitter and base regions much wider than a minority carrier diffusion length (non-transparent emitter) [2]. Jain and Muralidharan [8] derived the important result that, under normal conditions and with a wide base, the asymptotic value of the slope of the open-circuit voltage decay still depended on the minority carrier lifetime in the base region. Hence the method can be used to measure base lifetimes even with non-ideal emitters provided that the base region is wide.

Figure 5 shows calculated open-circuit voltage decay curves for various ratios of the dark current of the cell carried by the emitter and the base for the wide base case. In the simplest case the dark current carried by the emitter is zero ($J_E/J_B = 0$) and the curve reverts to the ideal curve of Section 2. The major effect of low emitter injection efficiency is to cause a more rapid initial decay while the slope of the decay after this initial region is not greatly affected. In practice, this latter section of the decay would be more difficult to detect as the injection efficiency decreased since it would be more likely to be masked by the shunting and capacitance effects of Section 3.

On the basis of a charge control analysis, it has been suggested that the initial regions of the decay may contain information about minority carrier lifetimes in the cell emitter [11]. This suggestion has been rejected, presumably on the grounds that the initial decay regions are best avoided because of

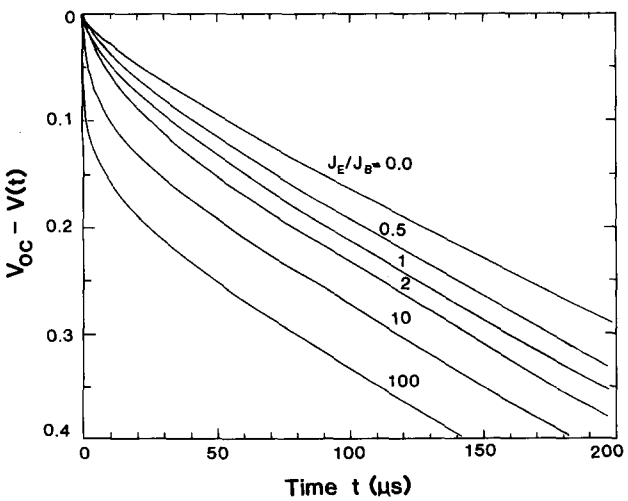

Fig. 5. Effect of non-ideal emitter properties on the open-circuit voltage decay of wide base solar cells ($\tau_E = 0$; $\tau_B = 20$ μs). The main effect is in the initial regions of the decay.

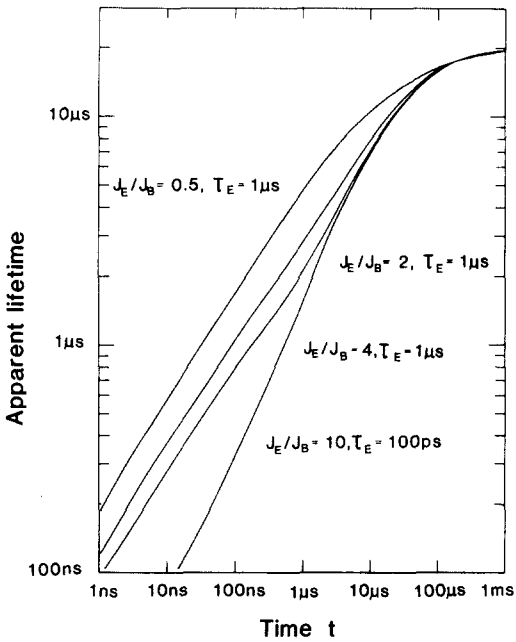

Fig. 6. Apparent lifetime calculated from curves as in Fig. 5 as $kT/(q \times \text{slope})$ for various emitter properties ($\tau_B = 20$ μs). In no case was there any indication that the emitter lifetime could be extracted from the decay curves.

non-linear contributions from the base decay [8]. However, the possibility that base and emitter decays may in some cases be sufficiently decoupled that the rapid initial decay region may contain a small linear section determined by the emitter lifetime has not been seriously examined. Such a linear region could easily be detected by the differential method of Section 4.

To examine this possibility theoretically, the differential of calculated curves such as those in Fig. 5 was also calculated as was the corresponding "lifetime" (kT/q multiplied by the inverse of the differential). Figure 6 shows representative results. In none of the cases examined was it possible to detect an inflection in the lifetime curve in the initial decay region at a lifetime value corresponding to the simulated emitter lifetime. This supports the original contention [8] that the initial regions of the open-circuit voltage decay do not contain useful lifetime information and are best ignored.

It should be noted, however, from Fig. 5 that the open-circuit voltage decay curve does contain information on the injection efficiency of the cell emitter. This information is only likely to be extracted when the injection efficiency is low (0.3 or less).

7. Finite emitter and base widths

The analysis of the effects of the emitter on the open-circuit voltage decay has recently been extended to include a wide variety of effects such

as finite emitter width, emitter fields due to doping gradients and surface recombination combined with finite base width [9]. This vast generalization was justified by the demonstration [8] that the emitter response is much faster than that of the base, allowing a quasi-static treatment of the emitter region [9].

With this simplification the problem essentially reduces to solving for the transient behaviour in the base region subject to boundary conditions formulated in terms of an effective recombination velocity not only at the rear contact to this region but also at the edge of the depletion layer bounding the other side of this region. The results of an independent analysis of this case developed for the interpretation of the open-circuit voltage decay in metal–insulator–semiconductor solar cells are given below.

If the effective recombination velocity at the edge of the deflection region is expressed as S_1 and that of the rear of the cell is expressed as S_2, then from quasi-static considerations S_1 will be given by J_{0e}/qn_B where J_{0e} is the contribution of the emitter to the diode saturation current density and n_B is the equilibrium value of the minority carrier concentration in the base at the edge of the depletion region. The lifetime measured from the asymptotic value of the decay is given by $\tau_B/(1+\phi^2)$ where τ_B is the actual base lifetime and ϕ is the first positive root of the equation

$$\left(\phi - \frac{S_1 S_2}{\phi}\frac{L_B^2}{D_B^2}\right)\tan\left(\frac{W\phi}{L_B}\right) = \frac{(S_1+S_2)L_B}{D_B} \tag{16}$$

Perhaps not surprisingly, the effect of a non-ideal emitter will be, in general, to accelerate the open-circuit voltage decay. For a device with a low recombination velocity rear contact ($S_2 \to 0$), eqn. (16) reduces to

$$\phi \tan\left(\frac{W\phi}{L_B}\right) = \frac{S_1 L_B}{D_B} \tag{17}$$

This is identical with eqn. (13) except that the recombination velocity applies at the opposite side of the base region. ϕ will increase from zero to $\pi L_B/2W$ as S_1 increases from zero to infinity. The rate of decay of the open-circuit voltage will increase as $1+\phi^2$. A practical example corresponding to the above case would be a cell with good bulk lifetimes and an effective back-surface field but with its open-circuit voltage limited by the properties of the diffused emitter.

For the opposite case of a high recombination velocity rear contact ($S_2 \to \infty$), eqn. (16) reduces to

$$\tan\left(\frac{W\phi}{L_B}\right) = -\frac{\phi D_B}{L_B S_1} \tag{18}$$

ϕ will increase from $\pi L_B/2W$ to $\pi L_B/W$ as S_1 increases from zero, again accelerating the decay.

For a wide base diode, ϕ will be small (less than $\pi L_B/W$) regardless of the values of S_1 and S_2. This allows a slight generalization of the results of Section 6. For a wide base cell the open-circuit voltage decay curve approaches a linear slope determined by the base lifetime regardless of emitter properties. The emitter properties would influence the early sections of the decay as in Section 6.

8. High injection

To minimize the junction capacitance and shunting effects of Section 3, the cell may be strongly forward biased. This can lead to high injection in the base of the cell, particularly when this region is lightly doped. Under high injection, calculation of ideal decay curves is complicated by the fact that not only junction voltages but also Dember voltages across the bulk regions have to be considered because of differences in electron and hole mobilities [12]. Additionally, ambipolar quantities which depend on injection level have to be used to describe carrier dynamics [5].

For the ideal case corresponding to that described in Section 2 the parameter f of eqns. (5) and (6) will be identically equal to 2 under high injection [13] and will reduce to unity under low injection in the quasi-static approximation. The effect of finite thickness and that of recombination at the rear boundary of the lightly doped region and in the emitter will accelerate the decay as in the lightly doped case except that ambipolar terms would be used in the corresponding equations.

For a constant base lifetime the expected behaviour of the open-circuit voltage decay would be to approach a linear decay under high injection conditions. As the transition to low injection was made, a second linear decay region would be entered but with a decay slope only half as steep. Experimentally, virtually every published result for open-circuit voltage decay in silicon originally biased into high injection shows just the opposite behaviour [2, 5, 12 - 16]. This was also confirmed by our experiments. A typical result for a low resistivity base is shown in Fig. 7. The rate of decay is relatively slow down to a voltage close to where the high injection to low injection transition is expected (0.317 V in the present device). Below this voltage the decay is much *quicker*.

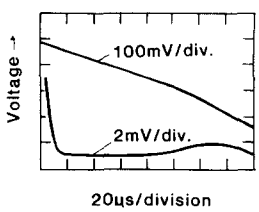

Fig. 7. Experimental decay for a 2000 Ω cm diode originally biased into high injection ($\tau_B \approx 48$ μs). The *increase* in slope at the voltage where the transition to low injection is expected (about 0.32 V) should be noted. The differentiator output is also shown (lower curve).

There have been three explanations proposed for this type of behaviour. One explanation is that the accelerated decay at low voltages is due to a shunting effect, as described in Section 3, as a result either of surface leakage [15] or of a surface recombination level [5]. Some of our experimental results support this interpretation. A second possible explanation is that the curves merely reflect an actual change in lifetime with increasing injection level by a factor typically of about 8 [12 - 14]. This is not unreasonable. For example, changes in the occupation statistics of gold recombination levels with increasing injection level are calculated to increase the bulk lifetime by a factor of 25 [17]. A more recent explanation [18] has been in terms of a saturation of the decay at high injection conditions, giving the "hump" in Fig. 7. This explanation does not stand up to critical examination. Experimental curves differ markedly from those derived with this theory. From the theoretical point of view, saturation of this type is calculated only when the junction potential barrier is forced to a small fraction of the thermal voltage kT/q. This is only likely to occur at very large current densities. For example, even at an enormous current density of 10^4 A cm^{-2}, two representative studies [19, 20] show that the junction potential barrier is still several times kT/q. The analysis [18] also has the limitation of equating the junction voltage to the terminal voltage ignoring Dember voltages.

9. Experimental results

9.1. Effect of finite base width

To investigate the effect of finite base widths on open-circuit voltage decay measurements, silicon wafers from the same batch were chemically thinned to different thicknesses in the 150 - 270 μm range and diodes were fabricated on them. Lower bounds on apparent diode lifetimes were then measured using the compensated differential open-circuit voltage decay technique of Section 4.

The theoretical variation in the measured lifetime τ_m would be as $\tau_B/(1 + \phi^2)$ where ϕ is the first positive root of eqn. (17). For the present experimental devices the recombination velocity S_2 at the rear contact is large (greater than D_B/L_B). In this case the solution of eqn. (17) simplifies for two extreme values of S_1, the effective recombination velocity of the emitter (Section 7). For small S_1, corresponding to high emitter injection efficiencies, ϕ approaches $\pi L_B/2W$ while for large S_1, corresponding to poor emitters, ϕ approaches $\pi L_B/W$ (Section 7). In both cases

$$\frac{1}{\tau_B} = \frac{1}{\tau_m} - \frac{\pi^2 D_B}{gW^2} \tag{19}$$

where $g = 1$ for a poor emitter and $g = 4$ for a good emitter. Hence, plotting $1/\tau_m$ *versus* $1/W^2$ might be expected to give data points lying within a region bounded by lines of slope $\pi^2 D_B$ and $\pi^2 D_B/4$.

Figure 8 shows experimental measurements for 26 diodes fabricated on thinned 0.1 Ω cm boron-doped wafers plotted as described above. The data

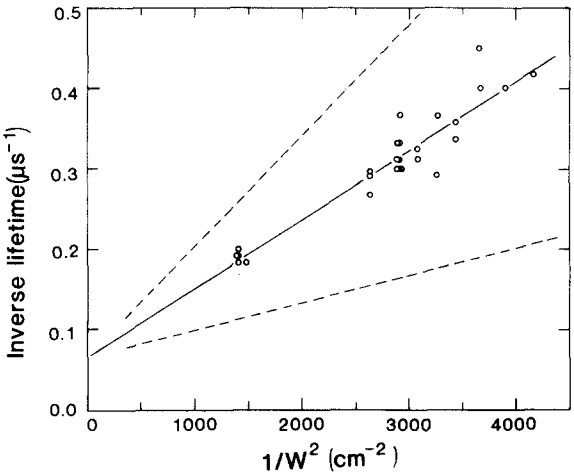

Fig. 8. Plot of experimentally measured lifetimes for various substrate thicknesses. The inverse of the measured lifetime is plotted against the square of the inverse base width: — — —, theoretical bounds; ——, least-squares fit to the experimental data (correlation coefficient, 0.95).

can be reasonably well fitted by a straight line of slope 85.87 $cm^2\ s^{-1}$ and a value of base lifetime τ_B of 15.5 μs (the correlation coefficient equals 0.95).

This result is in good qualitative agreement with theory. If we assume that the electron minority carrier diffusion coefficient D_B has the same value (14 $cm^2\ s^{-1}$) as the electron majority carrier diffusion coefficient in material of the same doping level, then the experimental value of g in eqn. (19) will be 1.6, intermediate between the limiting values of 1 and 4. The relatively low value of g suggests that S_1 must be comparable with D_B/L_B. From independent dark current–voltage characteristics the best estimate of S_1 for these devices is $2D_B/L_B$.

Actual base lifetimes τ_B could be calculated from the measured lifetimes τ_m as $\tau_m(1+\phi^2)$ by using eqn. (17) and assigning values to the parameters D_B, S_1 and S_2. Figure 9 shows the calculated results with $D_B = 14\ cm^2\ s^{-1}$, $S_1 = 2D_B/L_B$ and $S_2 = 100D_B/L_B$. The converted data gave a mean value of τ_B of 13.4 μs with a standard deviation of 2.7 μs. There appeared to be some dependence of τ_B on thickness. This could be an actual dependence or could be due to variations in the parameter values from those assumed above. The apparent thickness dependence would be reduced if D_B, S_1 or S_2 were increased above their assumed values.

The non-linearity of the ideal decay (Section 2) would cause the procedure above to underestimate τ_B, particularly for wide base diodes. Although it is possible to correct for this effect in wide base diodes [3], it would be very difficult to do this for the narrow base diodes of this section. The correction, in any case, would be smaller because of a theoretical increased linearity of decay for narrow base devices [7].

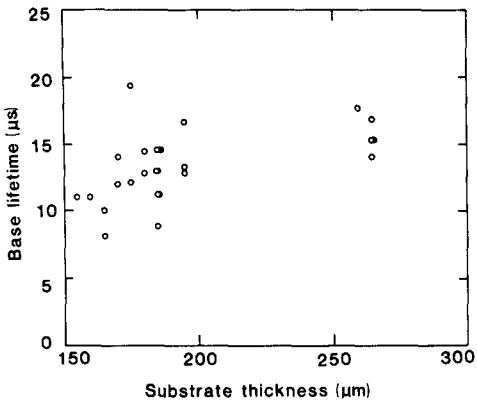

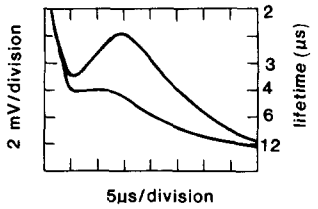

Fig. 9. Actual base lifetimes for the measurements of Fig. 6 as calculated from eqn. (17).

Fig. 10. Uncompensated and compensated differential open-circuit voltage decay measurements on a commercial terrestrial cell ($\tau_B \approx 6$ μs; $C_C = 1.7$ μF).

9.2. Terrestrial cells

Figure 10 shows the differential of the open-circuit voltage decay of a commercial terrestrial cell before and after compensation. As with most solar cells tested, this device had a relatively low shunt resistance and required a compensating capacitance to increase the accuracy of the reading. The forward bias current was set at approximately the solar current output for this and the following cells.

From the compensated curve a minimum bound on the cell lifetime is 4.1 μs. This cell did not have a back-surface field so that $4W^2/\pi^2 D_B$ represents an upper bound on the measured lifetime (12.1 μs). From eqn. (14) a better estimate of the lifetime is

$$\frac{1}{\tau_B} = \frac{1}{4.1\ \mu s} - \frac{1}{12.1\ \mu s}$$

This gives a value of 6.2 μs. Reference 3 describes a method of placing an upper bound on the lifetime which gives a value of 8.3 μs for this device.

9.3. Space cells

Figures 11 and 12 show the differentials of the open-circuit voltage decays for two space cells which exhibited interesting behaviour. The first cell was a commercial "violet" cell but with a double-layer antireflection coating. It had an excellent air mass 0 efficiency of 14.0% with an output current density greater than 40 mA cm^{-2} despite approximately 8% grid coverage. Notwithstanding this excellent performance, open-circuit voltage decay measurements indicated relatively low minority carrier lifetimes. Proceeding as in Section 9.2, a lower bound of 3.9 μs could be placed on the lifetime while the upper bound was calculated to be 7.6 μs. The high

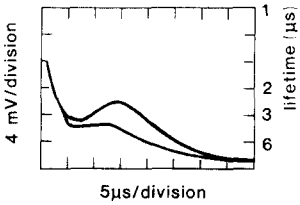

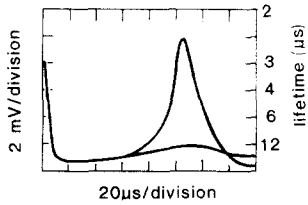

Fig. 11. Differential open-circuit voltage decay measurements on a high performance "violet" space cell ($\tau_B \approx 6$ μs; $C_C = 1$ μF).

Fig. 12. Differential open-circuit voltage decay measurements on a space cell with an excellent IR response ($\tau_B \approx 40$ μs; $C_C = 3$ μF). (The measurements showed that this device had an effective back-surface field.)

current output of this cell would have to be attributed to the good optical design of the cell rather than to good material properties.

The second cell was supplied by the Lewis Research Center, National Aeronautics and Space Administration. It had an excellent red response, close to the best that we have observed for a non-textured cell from any source. Figure 12 shows the differential of the open-circuit voltage decay before and after compensation was attempted. The lower bound on the lifetime in this device was measured at 32 μs, much higher than $4W^2/\pi^2 D_B$ (10.5 μs). Hence, from Section 5, this device has an effective back-surface field. From the cell saturation current density an upper bound of 250 cm s^{-1} is placed on the rear contact recombination velocity. Since $SW \ll D_B$, eqn. (15) can be used to place an upper limit on the base lifetime of 44 μs.

An interesting feature of this cell was that the measured lifetime decreased with decreasing injection level. At solar current densities the lifetime was calculated to lie in the range 32 - 44 μs as described above. At one-tenth of this current density, the corresponding range was 22 - 27 μs. This behaviour is evident in Fig. 12 as an increasing differentiator output when a time of between 20 and 60 μs has elapsed.

10. Conclusion

Recent experimental developments [3] have improved the reliability and accuracy of the open-circuit voltage decay method when used to measure minority carrier lifetimes in solar cells. Recent theoretical developments have improved the ability to interpret the experimental results. The effects of shunt resistance, junction capacitance and recombination, finite base width, non-ideal emitter properties and high injection are now well understood.

The compensated differential approach described is particularly well suited to placing lower bounds on lifetimes in completed cells. In some cases the upper bounds will not be appreciably higher than these lower bounds and actual lifetimes can be accurately estimated directly from the voltage decay measurement. In other cases, additional information will be required about the cell structure before useful upper bounds can be imposed.

In this paper these recent experimental and theoretical developments with the open-circuit voltage decay method have been summarized in a concise and unified manner with particular emphasis placed on their relevance to solar cell measurements.

Acknowledgments

Calculations for the various theoretical curves in this paper were done by Erik M. Keller. I also acknowledge the collaboration of Andrew W. Blakers in the experimental study of finite base widths.

This work was supported by the Australian Research Grants Scheme. The Joint Microelectronics Research Centre is funded by the Australian Commonwealth Programme for the Promotion of Excellence in Research.

References

1 B. R. Gossick, *Phys. Rev., 91* (1953) 1012.
2 S. R. Lederhandler and C. J. Giacoletto, *Proc. IRE, 43* (1955) 477.
3 M. A. Green, Minority carrier lifetimes using compensated differential open circuit voltage decay, *Solid-State Electron.*, to be published.
4 J. E. Mahan and D. C. Barnes, *Solid-State Electron., 24* (1981) 989.
5 L. W. Davies, *Proc. IEEE, 51* (1963) 1637.
6 S. R. Dhariwal and N. K. Vasu, *Solid-State Electron., 24* (1981) 915.
7 R. Muralidharan, S. C. Jain and U. Jain, *Sol. Cells, 6* (1982) 157.
8 S. C. Jain and R. Muralidharan, *Solid-State Electron., 24* (1981) 1147.
9 U. C. Ray, S. K. Agarwal and S. C. Jain, *J. Appl. Phys., 53* (1982) 9122.
10 M. A. Green, *Sol. Cells, 7* (1982) 337.
11 F. A. Lindholm and C. T. Sah, *J. Appl. Phys., 47* (1976) 4203.
12 S. C. Choo and R. G. Mazur, *Solid-State Electron., 13* (1970) 553.
13 R. J. Bassett, W. Fulop and C. A. Hogarth, *Int. J. Electron., 35* (1973) 177.
14 P. G. Wilson, *Solid-State Electron., 10* (1967) 145.
15 R. J. Bassett, *Solid-State Electron., 12* (1969) 385.
16 R. G. Mazur, Carrier lifetimes in junction devices from open circuit decay measurements. In H. R. Huff and R. R. Burgess (eds.), *Semiconductor Silicon*, Electrochemical Society, Princeton, NJ, 1973.
17 H. Maes and C. T. Sah, *IEEE Trans. Electron Devices, 23* (1976) 1131.
18 V. K. Tewary and S. C. Jain, *Solid-State Electron., 25* (1982) 903.
19 H. K. Gummel, *Solid-State Electron., 10* (1967) 209.
20 H. Guckel and A. Demirkol, *Solid-State Electron., 25* (1982) 105.